Goal-oriented mesh adaptation for flux-limited approximations to steady hyperbolic problems

Dmitri Kuzmin, Matthias Möller

Institute of Applied Mathematics (LS III), Dortmund University of Technology
Vogelpothsweg 87, D-44227, Dortmund, Germany

Abstract

The development of adaptive numerical schemes for steady transport equations is addressed. A goal-oriented error estimator is presented and used as a refinement criterion for conforming mesh adaptation. The error in the value of a linear target functional is measured in terms of weighted residuals that depend on the solutions to the primal and dual problems. The Galerkin orthogonality error is taken into account and found to be important whenever flux or slope limiters are activated to enforce monotonicity constraints. The localization of global errors is performed using a natural decomposition of the involved weights into nodal contributions. A nodal generation function is employed in a hierarchical mesh adaptation procedure which makes each refinement step readily reversible. The developed simulation tools are applied to a linear convection problem in two space dimensions.

Key words: steady transport equations, flux limiting, a posteriori error estimates, duality argument, goal-oriented mesh adaptation

1. Introduction

In many numerical methods for hyperbolic conservation laws, flux or slope limiters are employed to ensure nonlinear stability and suppress spurious oscillations. The resulting nonlinear approximation is at least second-order accurate in regions of smoothness but reverts to a nonoscillatory low-order

Email addresses: kuzmin@math.uni-dortmund.de (Dmitri Kuzmin), matthias.moeller@math.uni-dortmund.de (Matthias Möller)

scheme in the neighborhood of discontinuities and steep fronts. Local mesh refinement makes it possible to achieve a crisp resolution of small-scale features. On the other hand, the computational cost can be reduced by coarsening the mesh elsewhere. A reliable a posteriori estimate of local errors is required to identify the mesh elements to be refined or coarsened.

The goal-oriented approach to error estimation [1, 3, 9, 16, 18] is applicable not only to elliptic PDEs but also to hyperbolic conservation laws [5, 6, 17]. In most cases, the error in the quantity of interest is estimated using the duality argument, Galerkin orthogonality, and a direct decomposition of the weighted residual into element contributions. The most prominent representative of such error estimators is the Dual Weighted Residual (DWR) method of Becker and Rannacher [3, 4]. The recent paper by Meidner *et al.* [14] is a rare example of a DWR estimate that does not require Galerkin orthogonality or information about the cause of its possible violation.

Kuzmin and Korotov [12] applied the DWR method to steady convection-diffusion equations and obtained a simple estimate of local Galerkin orthogonality errors due to flux limiting or other 'variational crimes.' In contrast to the usual approach, the weighted residuals are decomposed into nodal (rather than element) contributions. In regions of insufficient mesh resolution, the computable Galerkin orthogonality error comes into prominence. The mesh adaptation strategy to be presented below takes advantage of this fact.

This paper is organized as follows. First, the weak form of a linear model problem is introduced. Next, a goal-oriented error estimate is derived, the practical implementation of adaptive mesh refinement/coarsening is discussed, and a multidimensional flux limiter is presented. Finally, a two-dimensional convection equation is solved using a limited FEM discretization on an adaptive mesh containing both triangular and quadrilateral cells.

2. Galerkin weak form

Steady convective transport of a conserved scalar quantity u in a domain Ω with boundary Γ can be described by the linear hyperbolic equation

$$\nabla \cdot (\mathbf{v}u) = s \qquad \text{in } \Omega. \tag{1}$$

Here $\mathbf{v}$ is a stationary velocity field and s is a volumetric source/sink. Due to hyperbolicity, a Dirichlet boundary condition is imposed at the inlet

$$u = u_D \qquad \text{on} \quad \Gamma_{\text{in}} = \{\mathbf{x} \in \Gamma \,|\, \mathbf{v} \cdot \mathbf{n} < 0\}, \tag{2}$$

where $\mathbf{n}$ is the unit outward normal and u_D is the prescribed boundary data.

The weak form of the above boundary value problem can be written as

$$a(w,u) = b(w), \qquad \forall w. \tag{3}$$

For brevity, we refrain from an explicit definition of functional spaces. The bilinear form $a(\cdot,\cdot)$ and the linear functional $b(\cdot)$ are defined by

$$a(w,u) = \int_\Omega w\,\nabla\cdot(\mathbf{v}u)\,\mathrm{d}\mathbf{x} - \int_{\Gamma_{\mathrm{in}}} wu\mathbf{v}\cdot\mathbf{n}\,\mathrm{d}s, \tag{4}$$

$$b(w) = \int_\Omega ws\,\mathrm{d}\mathbf{x} - \int_{\Gamma_{\mathrm{in}}} wu_D\mathbf{v}\cdot\mathbf{n}\,\mathrm{d}s. \tag{5}$$

The inflow boundary conditions are imposed weakly via the surface integrals.

The differentiation of $\mathbf{v}u$ in (4) can be avoided using integration by parts

$$a(w,u) = \int_\Gamma wu\mathbf{v}\cdot\mathbf{n}\,\mathrm{d}s - \int_\Omega \nabla w\cdot(\mathbf{v}u)\,\mathrm{d}\mathbf{x}. \tag{6}$$

This representation implies that a discontinuous weak solution u is admissible. In linear hyperbolic problems of the form (1), singularities travel along the streamlines of $\mathbf{v}$. They may be caused by a jump in the value of s or u_D.

3. Global error estimates

Let u_h be a continuous function that may represent an approximate solution to (1)–(2) or a finite element interpolant of discrete nodal values. The numerical error $e = u - u_h$ can be measured using the residual of (3)

$$\rho(w,u_h) = b(w) - a(w,u_h). \tag{7}$$

Obviously, the value of $\rho(w,u_h)$ depends not only on the quality of u_h but also on the choice of w. In goal-oriented estimates, this weight carries information about the quantities of interest. The objectives of a numerical study are commonly defined in terms of a linear output functional, such as [17]

$$j(u) = \int_\Omega gu\,\mathrm{d}\mathbf{x} + \int_{\Gamma_{\mathrm{out}}} hu\mathbf{v}\cdot\mathbf{n}\,\mathrm{d}s, \qquad g,h\in\{0,1\}. \tag{8}$$

The piecewise-constant function g picks out a subdomain, for example, an interior or boundary layer, where a particularly accurate approximation to

u is desired. The selector h picks out a portion of the outflow boundary $\Gamma_{\text{out}} = \{\mathbf{x} \in \Gamma \,|\, \mathbf{v} \cdot \mathbf{n} > 0\}$, where the convective flux is to be controlled.

In order to estimate the error $j(e)$ in the numerical value of the output functional, consider the *dual* or *adjoint* problem [3, 4] associated with (3)

$$a(z, e) = j(e), \qquad \forall e. \tag{9}$$

The surface integral in (8) implies the weakly imposed Dirichlet boundary condition $z = h$ on Γ_{out} [17]. The error $j(e)$ and residual (7) are related by

$$j(u - u_h) = a(z, u - u_h) = \rho(z, u_h). \tag{10}$$

An arbitrary numerical approximation z_h to the exact solution z of the dual problem (9) can be used to decompose the so-defined error as follows

$$j(u - u_h) = \rho(z - z_h, u_h) + \rho(z_h, u_h). \tag{11}$$

If Galerkin orthogonality holds for the numerical approximation u_h, then $\rho(z_h, u_h) = 0$. Thus, the computable term $\rho(z_h, u_h)$ is omitted in most goal-oriented error estimates for finite element discretizations. However, the orthogonality condition is frequently violated due to numerical integration, round-off errors, slack tolerances for iterative solvers, and flux limiting.

Since the exact dual solution z is usually unknown, the derivation of a computable error estimate involves another approximation $\hat{z} \approx z$ such that

$$j(u - u_h) \approx \rho(\hat{z} - z_h, u_h) + \rho(z_h, u_h). \tag{12}$$

The magnitudes of the two residuals can be estimated separately as follows:

$$|\rho(\hat{z} - z_h, u_h)| \leq \Phi, \qquad |\rho(z_h, u_h)| \leq \Psi, \tag{13}$$

where the globally defined bounds Φ and Ψ are assembled from contributions of individual nodes or elements, as explained in the next section.

The reference solution $\hat{z}$ is commonly obtained from z_h using some sort of postprocessing. If $\rho(z_h, u_h) = 0$, then the estimate $j(u - u_h) \approx 0$ that follows from (12) with $\hat{z} = z_h$ is worthless, hence the need to compute $\hat{z}$ on another mesh or interpolate it using higher-order polynomials [12, 16]. On the other hand, the setting $\hat{z} = z_h$ is not only acceptable but also optimal for nonlinear flux-limited discretizations such that $j(u - u_h) \approx \rho(z_h, u_h) \neq 0$. In situations when the term $\rho(z - z_h, u_h)$ is nonnegligible, extra work needs to be invested into the recovery of a superconvergent approximation $\hat{z} \neq z_h$.

4. Local error estimates

The global upper bounds Φ and Ψ make it possible to verify the accuracy of the approximate solution u_h but the estimated errors in the quantity of interest must be localized to find the regions where a given mesh is too coarse or too fine. A straightforward decomposition of weighted residuals into element contributions results in an oscillatory distribution and a strong overestimation of local errors. In particular, the restriction of the term $\rho(z_h, u_h)$ to a single element Ω_k can be large in magnitude even if Galerkin orthogonality is satisfied globally (positive and negative contributions cancel out).

Following Schmich and Vexler [16], we decompose Φ and Ψ into local bounds associated with the nodes of the mesh on which z_h is defined. Let

$$z_h = \sum_i z_i \varphi_i, \tag{14}$$

where $\{\varphi_i\}$ is a set of Lagrange basis functions such that $\sum_i \varphi_i \equiv 1$ and

$$\hat{z} - z_h = \sum_i w_i, \qquad w_i = \varphi_i(\hat{z} - z_h). \tag{15}$$

The contribution of node i to the bounds Φ and Ψ is defined as in [12]

$$\Phi_i = |\rho(w_i, u_h)|, \qquad \Psi_i = |\rho(z_i\varphi_i, u_h)|. \tag{16}$$

If the residual is orthogonal to the test function φ_i, then $\Psi_i = 0$. A nonvanishing value of Ψ_i implies a local violation of Galerkin orthogonality.

The magnitude of $j(u - u_h)$ is estimated by the sum of local errors, i.e.,

$$\Phi = \sum_i \Phi_i, \qquad \Psi = \sum_i \Psi_i. \tag{17}$$

Finally, an optional conversion into element contributions is performed for mesh adaptation purposes. Introducing the continuous error function

$$\xi = \sum_i \xi_i \varphi_i, \qquad \xi_i = \frac{\Phi_i + \Psi_i}{\int_\Omega \varphi_i \, \mathrm{d}\mathbf{x}}, \tag{18}$$

the following representation of the total error $\eta = \Phi + \Psi$ is obtained [12]

$$\eta = \sum_k \eta_k, \qquad \eta_k = \int_{\Omega_k} \xi \, \mathrm{d}\mathbf{x}. \tag{19}$$

In a practical implementation, the midpoint rule is employed to calculate η_k.

5. Hierarchical mesh adaptation

Any numerical method can be used to compute the approximate solutions u_h and z_h on a given mesh. The process of mesh adaptation is based on the estimate of local errors (19). Elements that make the largest contribution η_k to the global error η are refined, and the flow solver is invoked to recompute numerical solutions on the new grid. This process continues until the global error becomes smaller than a prescribed tolerance, and/or the maximum number of refinement cycles has been reached. The computational cost can be reduced by coarsening the mesh in regions where the local error is much smaller than average. For simplicity, the adaptation algorithm is presented for 2D grids which may consist of triangles and quadrilaterals.

5.1. Refinement algorithm

Following Bank et al. [2], the elements marked for refinement are subdivided into four (triangular or quadrilateral) subelements. This procedure generates hanging nodes at edge midpoints if an element is refined while its neighbor remains unrefined. In this event, the opposite cell is split into transition elements, so as to make the mesh globally conformal. Admissible refinement patterns in two dimensions are depicted in Fig. 1. If transition elements are further subdivided, then the mesh quality may deteriorate. Therefore, all green cells are removed at the beginning of the next refinement step, as suggested in [2]. By construction, each local subdivision can be reversed in a unique way by combining the corresponding cells into the original macroelement and deleting the vertices at the edge midpoints.

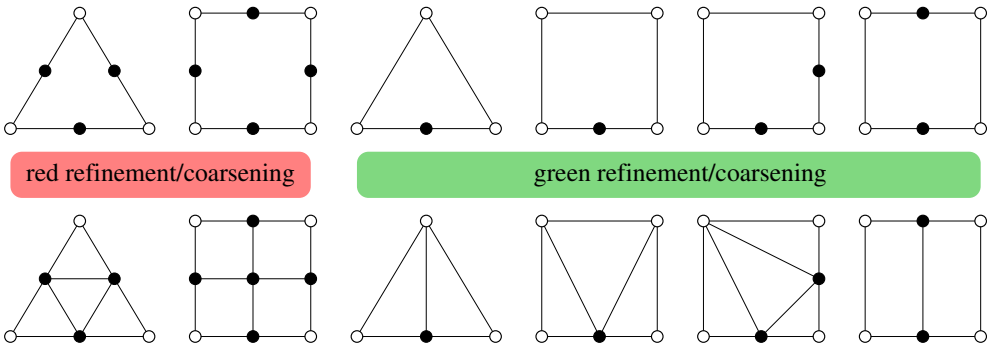

Figure 1: Refinement/coarsening patterns in two dimensions.

The hierarchical mesh adaptation procedure presented in [15] is a generalization of Hempel's [7] work to arbitrary meshes in two and three space dimensions. Let the sets of elements and vertices be denoted by $\mathcal{E} = \{\Omega_k\}$ and $\mathcal{V} = \{\mathrm{v}_i\}$, respectively. Consider an initial mesh $\mathcal{T}_h = (\mathcal{E}, \mathcal{V})$ free of hanging nodes. Following Hempel [7], each node is given a birth certificate that determines its age. The nodal generation function g is initialized by zero for all vertices belonging to $\mathcal{T}_h$ and updated during mesh refinement. If the new vertex v_i is created at the midpoint of an edge Γ_{kl} or in the interior of an element Ω_k, then its generation number is calculated as follows [15]:

$$g(\mathrm{v}_i) := \begin{cases} \max\limits_{\mathrm{v}_j \in \Gamma_{kl}} g(\mathrm{v}_j) + 1 & \text{if} \quad \mathrm{v}_i \in \Gamma_{kl} := \bar{\Omega}_k \cap \bar{\Omega}_l, \\ \max\limits_{\mathrm{v}_j \in \partial\Omega_k} g(\mathrm{v}_j) + 1 & \text{if} \quad \mathrm{v}_i \in \Omega_k \setminus \partial\Omega_k. \end{cases} \tag{20}$$

This is illustrated in Fig. 2 for a sequence of three nested meshes. Obviously, the number of subdivision steps required to construct a particular element coincides with the largest generation number evaluated at its vertices. It is worthwhile to store the nodal function g and use it to control the maximum number of refinements which may be different in different mesh regions.

5.2. Coarsening algorithm

The coarsening algorithm is designed to undo the subdivision of elements without changing the structure of coarser grid levels embedded in the sequence of nested meshes. Hence, the initial grid $\mathcal{T}_h$ can be recovered from

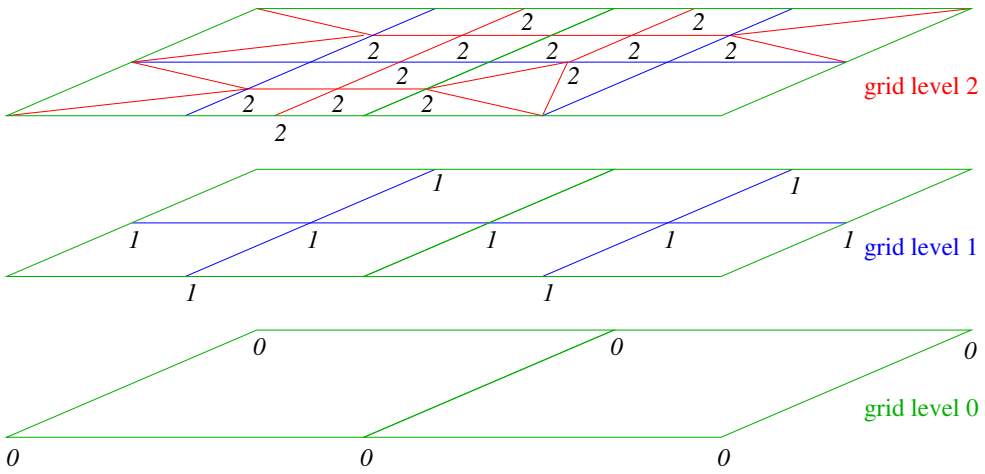

Figure 2: Mesh hierarchy with nodal generation numbers.

a (locally) refined one by combining groups of elements in *the* right order. It is worth mentioning that any mesh resulting from a sequence of refinement/coarsening steps can be constructed by pure element subdivision.

The nodal generation number (20) provides information about patches of cells that belong together, which makes it possible to rebuild the complete mesh hierarchy. Hempel [7] used this property of the generation function to develop a recursive vertex locking procedure for triangles in 2D. A revised algorithm applicable to arbitrary meshes was proposed in [15]. It is applied after marking the elements for refinement and before the actual subdivision.

Let the deletion indicator d be positive if a vertex is removable and non-negative otherwise. It is initialized by the nodal generation function $d \equiv g$ so that all vertices of the initial grid are locked unconditionally ($d(\mathrm{v}_i) = 0$). Unremovable nodes with $d > 0$ are locked step-by-step. If a cell is marked for refinement, its vertices need to be locked. Moreover, the vertices of an element Ω_k should be locked if the local error estimator η_k exceeds the coarsening tolerance and the element results from a regular subdivision (cf. Fig. 1: red refinement). This second check is necessary to make sure that the coarsening algorithm does not produce patterns of green elements that would not be created by pure mesh refinement. Next, generation numbers are compared in a loop over edges, and the older endpoint (if any) is locked

$$d(\mathrm{v}_i) := -|d(\mathrm{v}_i)| \quad \Leftrightarrow \quad \exists \Gamma_{ij} \text{ such that } g(\mathrm{v}_i) < g(\mathrm{v}_j). \tag{21}$$

This last step ensures that vertices are not removed if they belong to coarser grid levels. In practice, the preliminary set of removable nodes requires some post-processing to rule out the formation of invalid or undesirable element patterns (see [15] for technical details). Finally, all unlocked vertices and the connected elements/faces/edges are removed from the current mesh, and the macroelements/faces from the grid one level coarser are restored.

For example, consider the mesh hierarchy shown in Fig. 2 and let all cells present on level 2 be marked for coarsening. Nodes which belong to the initial mesh $\mathcal{T}_h$ are always locked ($d(\mathrm{v}_i) = 0$), while those with generation number 1 are locked by condition (21). Therefore, the elimination of red edges and corresponding vertices from level 2 yields the level 1 mesh.

6. Algebraic flux correction

In this work, the approximate solutions u_h and z_h are computed using a local extremum diminishing (LED) finite element scheme [10]. Within the

framework of algebraic flux correction, the linear system $Au = b$ that results from the standard Galerkin discretization of (1) is replaced by [10, 11, 13]

$$(A - D)u = b + \bar{f}(u), \tag{22}$$

where D is an artificial diffusion operator and $\bar{f}(u)$ is a limited antidiffusive correction. To enforce the M-matrix property for $A - D$, we take [10, 13]

$$d_{ii} = -\sum_{j \neq i} d_{ij}, \qquad d_{ij} = \max\{a_{ij}, 0, a_{ji}\}, \quad j \neq i. \tag{23}$$

The nonlinear correction term $\bar{f}(u)$ represents a sum of raw antidiffusive fluxes f_{ij} multiplied by solution-dependent correction factors $\alpha_{ij} \in [0, 1]$

$$\bar{f}_i = \sum_{j \neq i} \alpha_{ij} f_{ij}, \qquad f_{ij} = d_{ij}(u_i - u_j), \quad j \neq i. \tag{24}$$

It is easy to verify that the original system $Au = b$ is recovered for $\alpha_{ij} \equiv 1$.

By construction, the fluxes are skew-symmetric ($f_{ji} = -f_{ij}$), so mass conservation is maintained at the discrete level provided that $\alpha_{ji} = \alpha_{ij}$. Each pair of fluxes f_{ij} and f_{ji} can be associated with an edge of the sparsity graph and processed using efficient edge-based data structures [13].

For each pair of neighboring nodes i and j such that $a_{ji} \leq a_{ij}$, the computation of α_{ij} is based on the following sequence of algorithmic steps [10]

1. Compute the sums of positive/negative antidiffusive fluxes to be limited

$$P_i^+ := P_i^+ + \max\{0, f_{ij}\}, \qquad P_i^- := P_i^- + \min\{0, f_{ij}\}. \tag{25}$$

2. Compute the upper/lower bounds $Q_i^\pm$ to be imposed on the sums $P_i^\pm$

$$\begin{aligned} Q_i^+ &:= Q_i^+ + \max\{0, -f_{ij}\}, & Q_j^+ &:= Q_j^+ + \max\{0, f_{ij}\}, \\ Q_i^- &:= Q_i^- + \min\{0, -f_{ij}\}, & Q_j^- &:= Q_j^- + \min\{0, f_{ij}\}. \end{aligned} \tag{26}$$

3. Pick the nodal correction factor $R_i^\pm$ evaluated at the 'upwind' node i

$$R_i^\pm = \min\left\{1, \frac{Q_i^\pm}{P_i^\pm}\right\}, \qquad \alpha_{ij} = \begin{cases} R_i^+, & \text{if } f_{ij} > 0, \\ R_i^-, & \text{if } f_{ij} \leq 0. \end{cases} \tag{27}$$

The same correction factor $\alpha_{ji} := \alpha_{ij}$ is applied to the flux f_{ji} into node j located 'downwind' in the sense of the orientation convention $a_{ji} \leq a_{ij}$.

7. Numerical experiments

In this section, the presented high-resolution finite element scheme, goal-oriented error estimator, and hierarchical mesh adaptation algorithm are applied to a test problem from [8]. Consider equation (1) with $s \equiv 0$ and

$$\mathbf{v}(x,y) = (y,-x) \qquad \text{in} \quad \Omega = (-1,1) \times (0,1).$$

This incompressible velocity field corresponds to steady rotation about $(0,0)$.

The exact solution and inflow boundary conditions are given by [8]

$$u(x,y) = \begin{cases} 1, & \text{if } \ 0.35 \le \sqrt{x^2+y^2} \le 0.65, \\ 0, & \text{otherwise.} \end{cases}$$

The so-defined discontinuous inflow profile $(-1 \le x < 0,\ y = 0)$ undergoes circular convection and propagates along the streamlines of $\mathbf{v}(x,y)$ all the way to the outlet $(0 < x \le 1,\ y = 0)$, while its shape remains the same.

Let $j(u)$ be defined by (8) with $g = 1$ in $\omega = (-0.1, 0.1) \times (0,1)$ and $g = 0$ elsewhere. The function h is defined as the trace of g on Γ_{out}. The exact value of $j(u)$ is $6.04497\text{e}-02$. The solution shown in Fig. 3 (a) was computed by the FEM-LED scheme described in Section 6 on a uniform mesh of bilinear elements with spacing $h = 1/80$. Owing to algebraic flux correction, the resolution of the discontinuous front is remarkably sharp, and no undershoots or overshoots are observed. However, it is obvious that there is actually no need for such a high resolution beyond $x > 0.1$ if it is enough to have an accurate approximation in the small subdomain ω. Indeed, whatever is happening downstream of ω has no influence on the solution in this subdomain. This is illustrated by Fig. 3 (b) which shows the solution to the dual problem computed by the FEM-LED scheme on the same mesh.

Goal-oriented error analysis is performed using estimate (12) with $\hat{z} = z_h$. This setting implies that $\Phi = 0$ and $\eta = \Psi$ is the Galerkin orthogonality error caused by flux limiting. Remarkably, the resulting global estimates are in a good agreement with the exact error which is illustrated in Table 1 for different grid spacings. The sharpness of the obtained error estimates is measured using the absolute and relative effectivity indices [12]

$$I_{\text{eff}} = \frac{\eta}{|(j(u-u_h)|}, \qquad I_{\text{rel}} = \left| \frac{|(j(u-u_h)| - \eta}{|(j(u)|} \right|.$$

We remark that the value of I_{eff} is unstable and misleading when the denominator is very small or zero, and the evaluation of integrals is subject to

h	$\lvert j(u-u_h)\rvert$	$\eta(z_h,u_h)$	I_{eff}	I_{rel}
1/10	2.009555e-03	2.115012e-03	1.05	1.744541e-03
1/20	4.401534e-04	3.640322e-04	0.82	1.259248e-03
1/40	1.312391e-04	1.025215e-04	0.78	4.750662e-04
1/80	4.283158e-05	3.535738e-05	0.82	1.236433e-04
1/160	1.254089e-05	1.072697e-05	0.85	3.000709e-05

Table 1: Circular convection: exact vs. estimated global error.

rounding errors. The relative effectivity index I_{eff} is free of this drawback and exhibits monotone convergence as the mesh is refined (see Table 1).

The adaptive hybrid mesh presented in Fig. 4 is refined along the discontinuity lines of u but only until they cross the outflow boundary of ω. Using a finer mesh beyond the line $x = 0.1$ would not improve the accuracy of the solution u_h inside ω. The smallest mesh width is $h = 1/320$, which corresponds to more than 200,000 cells in the case of global mesh refinement.

Since the dual weight z_h contains built-in information regarding the transport of errors and goals of simulation, such error estimators furnish a better refinement criterion than, for example, error indicators based on gradient recovery [19]. In the latter case, unnecessary mesh refinement would take place along the discontinuities located downstream of the subdomain ω.

8. Conclusions

A goal-oriented error estimate was derived for nonlinear discretizations of a steady transport equation. The loss of Galerkin orthogonality in the process of flux limiting was shown to provide valuable feedback for mesh adaptation. A hierarchical mesh adaptation strategy was described and used to generate a locally refined hybrid mesh for circular convection in a 2D domain. Diffusive terms can be included using gradient recovery to stabilize the residuals and infer a proper distribution of local errors [12]. Further work will concentrate on goal-oriented error estimation for unsteady flow problems.

Acknowledgments

This research was supported by the German Research Association (DFG) under grant KU 1530/3-2. The authors would like to thank Dr. Sergey Korotov (Helsinki University of Technology), Prof. Boris Vexler and Dr. Dominik Meidner (Technische Universität München) for valuable comments.

(a) primal solution

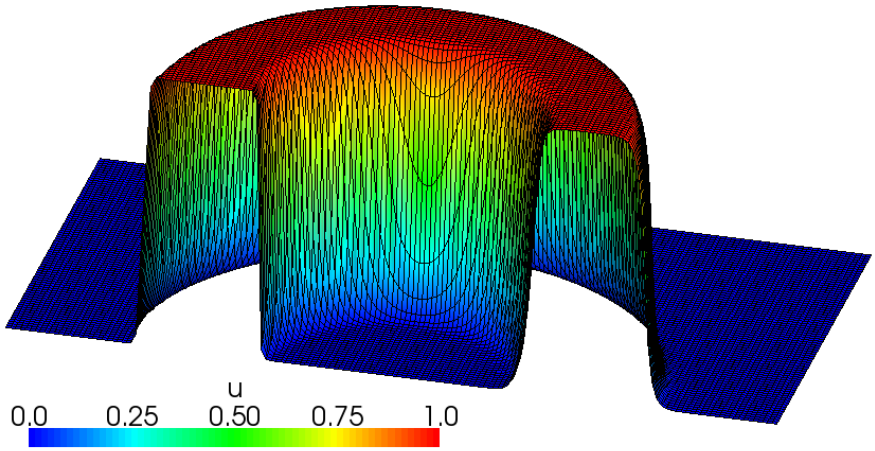

(b) dual solution

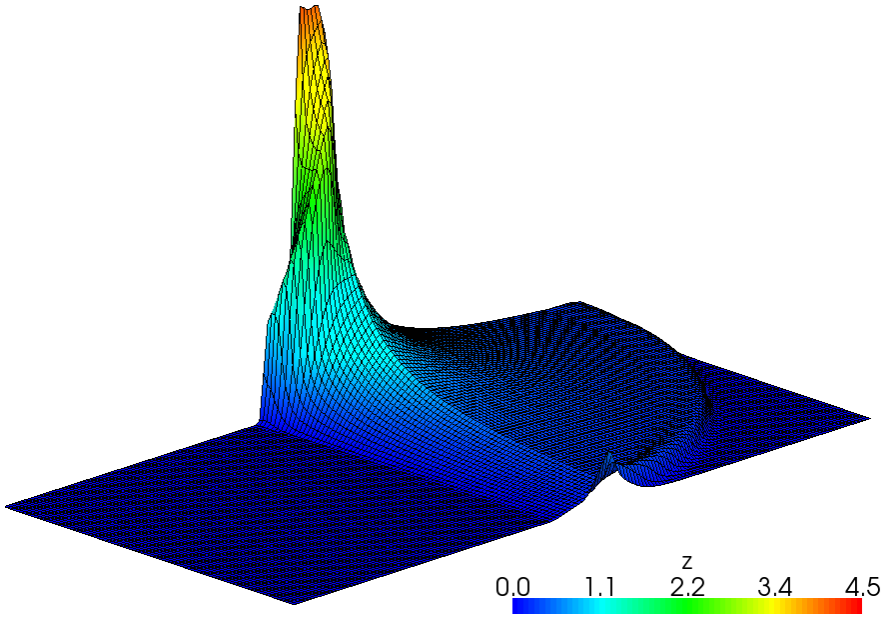

Figure 3: Circular convection: FEM-LED discretization, $h = 1/80$.

(a) primal solution

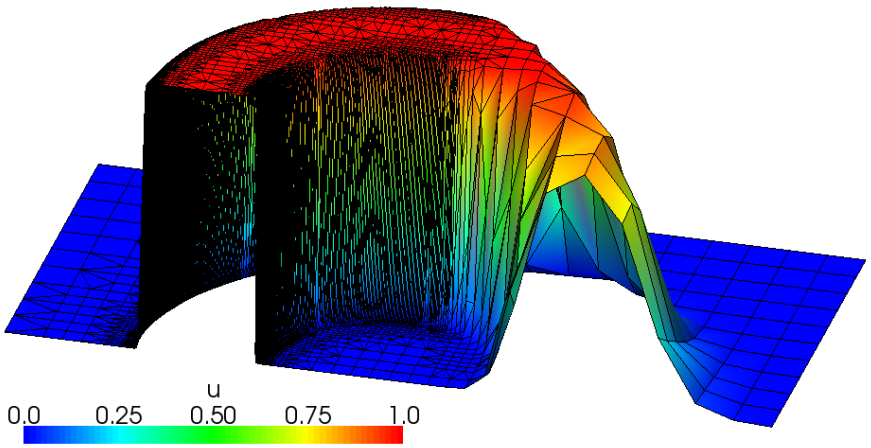

(b) computational mesh

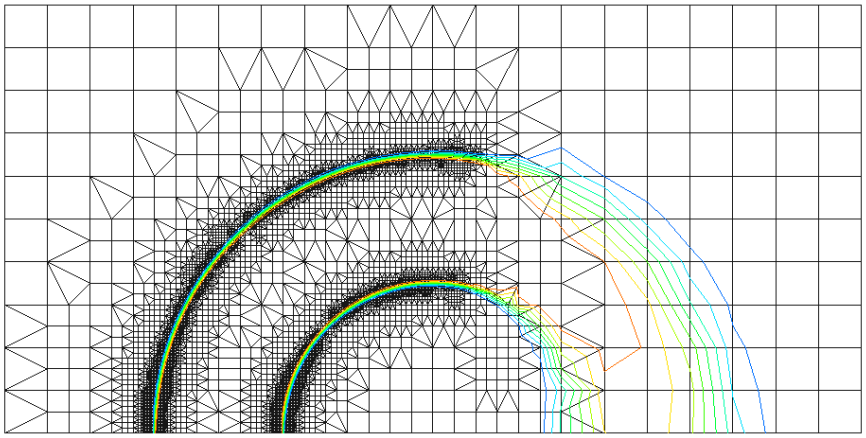

Figure 4: Circular convection: FEM-LED discretization, 5,980 cells.

References

[1] W. Bangerth and R. Rannacher, Adaptive finite element methods for differential equations. Lectures in Mathematics, ETH Zürich, Birkhäuser, 2003.

[2] R.E. Bank, A.H. Sherman and A. Weiser, Some refinement algorithms and data structures for regular local mesh refinement. In: R. Stepleman (eds.), *Scientific Computing, Applications of Mathematics and Computing to the Physical Sciences*, volume I of *IMACS Transactions on Scientific Computation*, Amsterdam, 1983, 3-17.

[3] R. Becker and R. Rannacher, A feed-back approach to error control in finite element methods: Basic analysis and examples. *East-West J. Numer. Math.* **4** (1996) 237–264.

[4] R. Becker and R. Rannacher, An optimal control approach to a posteriori error estimation in finite element methods. *Acta Numerica* **10** (2001) 1–101.

[5] R. Hartmann, Adaptive FE methods for conservation equations. In: H. Freistühler and G. Warnecke (eds.), *Hyperbolic Problems: Theory, Numerics, Applications*, ISNM **141**. Birkhäuser, Basel, 2001, 495-503.

[6] R. Hartmann and P. Houston, Adaptive discontinuous Galerkin finite element methods for nonlinear hyperbolic conservation laws. *SIAM J. Sci. Comput.* **24** (2002) 979–1004.

[7] D. Hempel, *Rekonstruktionsverfahren auf unstrukturierten Gittern zur numerischen Simulation von Erhaltungsprinzipien.* PhD thesis, University of Hamburg, 1999.

[8] M.E. Hubbard, Non-oscillatory third order fluctuation splitting schemes for steady scalar conservation laws. *J. Comput. Phys.* **222** (2007) 740–768

[9] S. Korotov, P. Neittaanmäki and S. Repin, A posteriori error estimation of goal-oriented quantities by the superconvergence patch recovery. *J. Numer. Math.* **11** (2003) 33–59.

[10] D. Kuzmin, Algebraic flux correction for finite element discretizations of coupled systems. In: E. Oñate, M. Papadrakakis, B. Schrefler (eds)

Computational Methods for Coupled Problems in Science and Engineering II, CIMNE, Barcelona, 2007, 653–656.

[11] D. Kuzmin, On the design of general-purpose flux limiters for implicit FEM with a consistent mass matrix. I. Scalar convection. *J. Comput. Phys.*, **219**, 513-531, (2006).

[12] D. Kuzmin and S. Korotov, Goal-oriented a posteriori error estimates for transport problems. *Math. Comp. Simul.* (2009), in press, doi:10.1016/j.matcom.2009.03.008.

[13] D. Kuzmin and M. Möller, Algebraic flux correction I. Scalar conservation laws. In: D. Kuzmin, R. Löhner, S. Turek (eds) *Flux-Corrected Transport: Principles, Algorithms, and Applications*. Springer, 2005, 155–206.

[14] D. Meidner, R. Rannacher and J. Vihharev, Goal-oriented error control of the iterative solution of finite element equations. *J. Numer. Math.* (2009), accepted.

[15] M. Möller, *Adaptive High-Resolution Finite Element Schemes*. PhD thesis, Dortmund University of Technology, 2008.

[16] M. Schmich and B. Vexler, Adaptivity with dynamic meshes for space-time finite element discretizations of parabolic equations. *SIAM J. Sci. Comput.* **30**:1 (2008) 369–393.

[17] C. Steiner and S. Noelle, On adaptive timestepping for weakly instationary solutions of hyperbolic conservation laws via adjoint error control. *Commun. Numer. Meth. Engrg.* (2009), in press, doi:10.1002/cnm.1183.

[18] P. Šolin and L. Demkowicz, Goal-oriented *hp*-adaptivity for elliptic problems. *Comput. Methods Appl. Mech. Engrg.* **193** (2004) 449–468.

[19] O.C. Zienkiewicz and J.Z. Zhu, A simple error estimator and adaptive procedure for practical engineering analysis. *Int. J. Numer. Methods Engrg.* **24**:2 (1987) 337–357.